Magnetic circular dichroism in core-level photoemission from Gd, Tb, and Dy in ferromagnetic materials

Elke Arenholz, Eduardo Navas, Kai Starke, Lutz Baumgarten, and Günter Kaindl
Institut für Experimentalphysik, Freie Universität Berlin, Arnimallee 14, D-14195 Berlin-Dahlem, Germany
(Received 10 August 1994)

Core-level photoemission (PE) spectra from magnetically ordered lanthanide materials display strong magnetic circular dichroism (MCD). Particularly large MCD effects were observed in $4f$ PE from Gd, Tb, and Dy, with the intensities of resolved $4f$ PE lines changing up to 62%. Substantial MCD effects were also found in $4d$ core-level PE. The perspectives of applying MCD in $4f$ PE as an element-specific tool for studies of surface and interface magnetism and as a sensor for the degree of circular polarization of soft x rays are discussed.

I. INTRODUCTION

The magneto-optical Kerr effect and Faraday effect are commonly used for studying magnetic materials by polarized visible light. Only recently, in 1986, an analogous effect in the x-ray region, magnetic circular dichroism in x-ray absorption (MCXD) was observed by Gisela Schütz and co-workers for the K-edge x-ray-absorption spectrum of magnetized Fe metal.[1,2] Later on, MCXD was also found for the absorption edges of various elements, in particular the "white-line" structures at the $L_{2,3}$ thresholds of lanthanide materials[3] and $3d$ transition metals.[4] The discovery of MCXD opened up the possibility for an element-specific analysis of magnetic moments in compound magnets and multilayers; today it is mainly used at the $L_{2,3}$ thresholds of $3d$ transition-metal materials,[4–9] which yield particularly large MCD asymmetries. In these cases, the white-line intensities change by up to 40% upon reversal of either sample magnetization or light helicity (photon spin).[8,10] These large MCD asymmetries have been shown to be useful for element-specific magnetic domain imaging.[11] Concurrent with these experimental developments of MCXD, quite rigorous theoretical descriptions have been given;[12–15] among them, the recently formulated sum rules[16,17] allow to separately derive the orbital and spin magnetic moments from the MCXD spectra.[18]

The obvious success of MCXD has stimulated the search for similar effects in photoemission (PE), motivated by the well-known merits of PE, namely high surface sensitivity and tuneable sampling depth by variation of the kinetic energy of the photoelectrons. Yet, from the absorption case it is clear that there are three important ingredients for magnetic circular dichroism. They can already be recognized in the simple one-electron picture by taking into account the spin polarization of the excited electron due to the inner-shell spin-orbit coupling (Fano-effect[19]) as well as the spin-split density of final states at and above the Fermi level.[20] These three ingredients are (i) exchange interaction as the driving force for long-range spin order; (ii) use of circularly polarized light with preferential propagation along the magnetic quantization axis; (iii) spin-orbit interaction providing the mechanism for an effective coupling between the angular momentum of the circularly polarized photon and the magnetically ordered electron spins.

The successful observation of MCD in PE was made for the $2p$ core-level spectrum of Fe metal,[21] where several percent MCD asymmetry can be found.[21–23] In this case, unlike absorption, the electron is excited into continuum states far above threshold that have negligible spin dependence and hence cannot act as a spin-filter analogous to the spin-polarized final states in case of photoabsorption. The relatively small MCD effects observed for the $2p_{1/2}$ and $2p_{3/2}$ core-level PE signals are due to exchange interaction between the magnetically ordered $3d$ electrons and the $2p$ core electrons ($\Delta E_{ex} \cong 0.5$ eV), causing a core-level exchange splitting into $|M_J\rangle$ sublevels.[24] Their relative intensities, given by the dipole-transition probabilities to continuum states, depend on the change of the M_J quantum number as a function of the relative orientation between photon spin and sample magnetization. The observed MCD effect is small compared to MCXD, mainly because the exchange splitting is smaller than the intrinsic width of the $2p$ core levels. This means that individual $|M_J\rangle$ components cannot be resolved. Larger MCD effects in transition metals might have been expected in PE from magnetic $3d$ band states, since the exchange interaction of these states is much larger than the lifetime width. However, the MCD effects were found to be of similar size as in core-level PE (with asymmetries up to $\cong 8\%$).[25,26] This is due to an inefficient transfer of the photon-momentum orientation to the (magnetically ordered) spin of the $3d$ electrons, caused by weak spin-orbit coupling and the well-known quenching of the orbital angular momentum in $3d$ transition metals.

The situation is entirely different for the localized $4f$ states in lanthanide (Ln) materials. Being closely bound inside the filled $5s$ and $5p$ shells, the $4f$ states essentially maintain their atomic character also in the solid state and normally do not contribute to chemical bonding. Crystal fields, which quench the orbital moment in $3d$ ferromagnets, have thus little effect on the Ln $4f$ orbitals; i.e., the larger orbital momenta exist also in the solid state. At each crystal-lattice site, the $4f$ spin-orbit coupling (of

0163-1829/95/51(13)/8211(10)/$06.00

typically 0.1 to 1.5 eV) aligns orbital and spin momentum according to Hund's rules. As a further direct consequence of their localized nature, the $4f$ electrons are subject to a relatively stronger Coulomb correlation than the $3d$ electrons in transition metals. This is beautifully reflected in the $4f$ PE spectra of lanthanide metals:[27] The energy-distribution curves of photoemitted $4f$ electrons typically show many lines corresponding to different correlation energies of the remaining electrons in the $4f^{n-1}$ PE final state. In the case of long-range ferromagnetic order, where the total $4f$ moments of all lattice sites are oriented parallel, the indirect exchange interaction primarily couples neighboring $4f$ spin moments. By spin-orbit coupling at each lattice site, also the orbital angular momenta assume long-range orientation. In PE experiments with circularly polarized light, the selection rule $\Delta M=\pm 1$ causes the excitation probability to depend on the relative orientation of the photon momentum and the $4f$ orbital momentum. Thus large MCD effects are expected in $4f$ PE from Ln materials, where PE multiplet lines with different final-state angular momenta can be resolved.[27]

In the present paper we report on the state of our studies of MCD in PE from $4f$ and $4d$ levels of lanthanide materials. After a detailed description of the experimental procedure in Sec. II, we present in Sec. III MCD-in-$4f$-PE spectra from monocrystalline Gd, Tb, and Dy metal films, revealing MCD asymmetries comparable with or even higher than those obtained by MCXD. Taking Gd as an example, it is demonstrated that the observed MCD in $4f$ PE can be described by an atomic model making use of dipole-selection rules in LS coupling. In Sec. IV, we report on the observation of MCD in $4d$ core-level PE from Gd; it is compared with the Fe $2p$ case reported previously.[21] The perspectives in applying the large MCD asymmetries in $4f$ PE as a magnetometer for lanthanide surfaces and thin films and as an x-ray polarimeter are demonstrated and discussed in Sec. V. Summary and outlook are given in Sec. VI.

II. EXPERIMENTAL DETAILS

The PE experiments were performed with circularly polarized soft x rays from two different monochromators at the Berliner Elektronenspeicherring für Synchrotronstrahlung (BESSY): The plane-grating SX700/III,[28] located at a bending magnet, and the U2-FSGM, behind a crossed undulator.[29] The SX700/III is equipped with two premirrors selecting synchrontron radiation from above or from below the storage-ring plane. It provides light with a high degree of circular polarization at photon energies exceeding $\cong 100$ eV, which are well suited for bulk-sensitive PE studies. S_3 is the Stokes parameter measuring the degree of circular polarization;[30] it is, e.g., $\cong 0.9$ at $h\nu=265$ eV for an off-plane angle of $\psi=0.9$ mrad.[31] For surface-sensitive measurements, we employed the crossed undulator, which supplies a high photon flux at lower energies with $S_3\cong 0.5$ around $h\nu=50$ eV.[29] At present, there is no alternative to the use of synchrontron radiation for circularly polarized soft x rays.

The preparation of clean and well-ordered monocrystalline Ln metals is a delicate matter. Due to the high chemical reactivity of Ln metals, contaminants of the bulk crystals, like O, H, and C can be hardly depleted by the usual UHV-sputter/anneal cycles.[32] Much cleaner samples are obtained by growing monocrystalline films in UHV, e.g., by vapor deposition of the Ln metal onto a suitable substrate. The base pressure in the experimental chamber used was $<3\times 10^{-11}$ mbar; during evaporation, it rose briefly to $<2\times 10^{-10}$ mbar. We used W(110) as a substrate, since it can be easily prepared, does not alloy with Ln metals, and allows the heavy Ln metals to grow on it by forming hexagonally close-packed (0001) surfaces. The lattice mismatch, which is $\cong 4\%$ in the case of Gd,[33] gives rise to some strain in monolayer-thin films, that is, however, released near the surface of a thick film.

In order to suppress the formation of islands during deposition, the substrate was kept at temperatures below 300 K, resulting in flat films (80 to 150 Å thick) with little lateral order. Well-ordered films of Gd, Tb, and Dy, as confirmed by low-energy-electron diffraction (LEED), were obtained by subsequent annealing for 5 min at $T_{an}=600-900$ K, with T_{an} depending on the thickness of the film.[34] The intensities of the well-known d-like surface states of the Ln metals in the valence-band PE spectra just below the Fermi level were used as a sensitive measure of film quality. The film thickness was monitored by a quartz microbalance and calibrated via the relative intensities of the $4f$ PE lines from W and from the Ln. Chemical cleanliness was checked via $1s$ PE intensities of O and C as well as by the O $2p$ PE signal; in the latter case, O_2 exposures as low as $\frac{1}{100}$ of a Langmuir could be easily monitored.

The experimental geometry is shown schematically in Fig. 1. The circularly polarized light was incident at an angle of 15° with respect to the film plane, and the photoelectrons were collected around the surface normal by a hemispherical electron-energy analyzer with a moderate angular resolution of ±10°. In this geometry, an almost pure MCD effect is measured despite the partially angle-resolved electron detection.[35]

The PE spectra were taken with the films remanently magnetized in plane. Remanent magnetization was compulsory, since an application of external fields is not com-

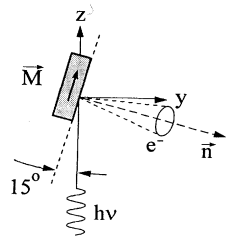

FIG. 1. Schematics of the experimental geometry. The Ln films were remanently magnetized in plane, with the circularly polarized x-ray beam incident at an angle of 15° with respect to the film plane. The photoelectrons were detected normal to the surface.

patible with high-resolution low-energy PE. The in-plane magnetization was checked *in situ* by magneto-optical Kerr effect (MOKE) studies, using a MOKE setup that has been described elsewhere.[36]

Note that these PE experiments are quite simple as far as energy and angular resolution are concerned, while they are quite demanding in two other respects: (i) Many of the Ln films have to be cooled to rather low temperatures due to low Curie temperatures (e.g., Ho with $T_c \cong 20$ K), while the W(110) substrate is flashed to $\cong 2000$ K for cleaning. This requires an optimized compromise regarding the thermal contact between substrate and cooling stage. In this respect, Gd, which has the highest spin moment ($7\mu_B$) and the highest Curie temperature ($T_c \cong 290$ K) of all Ln metals, represents the simplest case. (ii) All magnetic Ln metals, except for Gd and Eu have a nonspherical $4f$ charge distribution, which—by interaction with the low-symmetry hexagonal crystal field—accounts for the well-known and quite large single-ion anisotropy energies. They give rise to high coercive fields that do not readily allow to change the sample magnetization by small external fields. For Gd (half-filled $4f$ shell), the orbital angular momentum and thus the single-ion anisotropy vanishes. The coercive fields are therefore small enough to allow the sample to be magnetized by field pulses (duration <1 s) of only a few 100 A/cm applied through a closeby selenoid. This easy magnetization procedure in case of Gd allows us to measure a pair of MCD spectra (both magnetization directions for a fixed photon spin) in a quasisimultaneous way by reversing the magnetization pulse at each electron-kinetic energy point. By this differential measurement of the MCD signal, long-term instabilities of the apparatus (e.g., due to changes of the electron-storage ring) cancel.

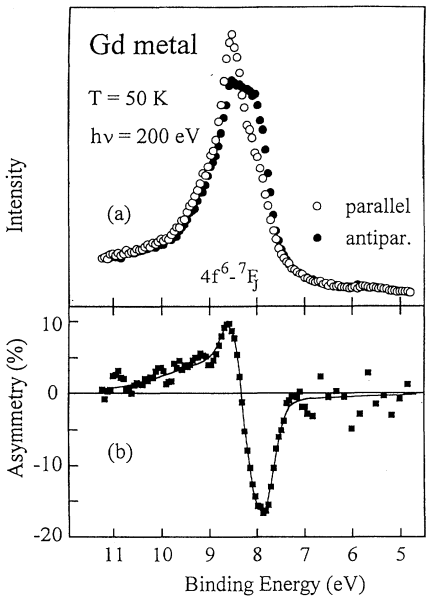

FIG. 2. (a) Gd $4f$ PE spectra ($h\nu = 200$ eV) of a remanently magnetized Gd(0001)/W(110) film (80 Å thick; $T = 50$ K). Open (filled) dots represent parallel (antiparallel) orientation of photon spin and sample magnetization. (b) The normalized intensity asymmetry, calculated from the raw data in (a), amounts up to 17%.

III. MCD IN $4f$ PHOTOEMISSION

A. Gadolinium metal

$4f$ PE spectra from a magnetized 80-Å-thick Gd(0001) film at $T \cong 50$ K, obtained with circularly polarized light from the SX700/III monochromator, are shown in Fig. 2(a). For nearly parallel orientation of photon spin and sample magnetization, the $4f^6 - {}^7F_J$ final-state multiplet assumes a peaked shape, which changes into a rounded shape upon reversal of magnetization. The normalized intensity asymmetry, $(I\uparrow\uparrow - I\downarrow\uparrow)/(I\uparrow\uparrow + I\downarrow\uparrow)$, calculated from the raw experimental data, amounts up to 17% [Fig. 2(b)]. It is considerably larger than the MCD asymmetries obtained in PE from $3d$ transition metals. An identical MCD effect was observed for a given magnetization direction when the photon helicity was reversed (spectra now shown here).[37]

Due to the localized nature of the $4f$ orbitals, we expect that the observed MCD effect can be described in an atomic model. In the following we derive, using the LS-coupling scheme, the intensities of the seven ${}^7F_J$ final-state PE-multiplet components for the two cases of parallel and antiparallel orientation of photon spin and sample magnetization. We shall see that the MCD effect is a simple consequence of the dipole-selection rule $\Delta M = +1$ or $\Delta M = -1$, depending on whether photon spin and sample magnetization are parallel or antiparallel, respectively.

The Gd ground state, ${}^8S_{7/2} - |J,M\rangle$, is characterized by the total angular momentum quantum number $J = 7/2$ and the magnetic quantum number M. The ground state is connected via the dipole-selection rules $\Delta J = 0, \pm 1$ and $\Delta M = \pm 1$ with the complete final state $|J',M'\rangle$, obtained by coupling all angular momenta of the ${}^7F_J$ PE final state ($L = 3, S = 3$) and of the detected photoelectron. In order to calculate the MCD effect, i.e., the influence of the ΔM selection rule on the intensities of the final-state PE-multiplet components, we first use the complete final state and then decouple the angular momentum of the photoelectron. For the photoelectron, we only consider $4f \rightarrow \varepsilon g$ transitions, since contributions from $4f \rightarrow \varepsilon d$ are expected to be small for PE final states far above the continuum threshold.[38]

In a first step, we consider the four complete final states $|J',M'\rangle$ that can be reached from the fully magnetized ground state $|J = 7/2, M = -7/2\rangle$ (see Table I): For $\Delta M = -1$, the only possible transition is $\Delta J = +1$, whereas all three ΔJ transitions are allowed for $\Delta M = +1$. By help of the Wigner-Eckart theorem, we separate the ΔM dependence of the transition probability $|\langle J'M'|P^{\Delta M}|JM\rangle|^2$ (with $P^{\Delta M}$= dipole operator) and hereby obtain statistical weights for all four transitions given in the last column of Table I. While $|J' = 9/2\rangle$ is the only allowed state for $\Delta M = -1$, this state is hardly

TABLE I. Relative dipole transition probabilities for Gd from the fully magnetized ground state $|7/2,-7/2\rangle$ to the four allowed total final state $|J',M'\rangle$. The relative weights have been calculated in the LS-coupling scheme; they clearly reflect a dominance of transitions with $\Delta J=-\Delta M$.

ΔM	$\lvert J',M'\rangle$	ΔJ	Relative weight
+1	$\lvert 9/2,-5/2\rangle$	+1	1/36
+1	$\lvert 7/2,-5/2\rangle$	0	2/9
+1	$\lvert 5/2,-5/2\rangle$	−1	3/4
−1	$\lvert 9/2,-9/2\rangle$	+1	1

reached by the $\Delta M=+1$ transitions, with a negligible weight of 1/36. Most of the $\Delta M=+1$ transitions (3/4) reach the $|J'=5/2\rangle$ state, reflecting a dominance of transitions with $\Delta J=-\Delta M$. This dominance is essential for the occurrence of MCD in PE, as shown in the following.

In a second step we decouple the photoelectron momenta ($l=4$, $s=\frac{1}{2}$) from the final state $|J',M'\rangle$, obtaining the intensity distribution over the individual ^7F_J multiplet components of the PE final state. It is drastically different for the different ΔJ: In case of $\Delta J=-1$, the $J=6$ final-state component carries about 50% of the intensity, whereas it assumes only about 5% in case of $\Delta J=+1$.

The results of this atomic-multiplet calculation are shown graphically in Fig. 3(a) for $\Delta M=+1$ (parallel orientation) and (b) for $\Delta M=-1$ (antiparallel orientation). The values agree well with the results of recent intermediate-coupling calculations by van der Laan and Thole[38] carried out with the Cowan computer code.[39] Also included in Fig. 3 are the experimental spectra from Fig. 2, however, normalized to complete circular polarization of the photon beam ($S_3=1$), in order to facilitate a comparison. Note the good qualitative agreement between the shapes of the normalized experimental spectra and the theoretical multiplets.

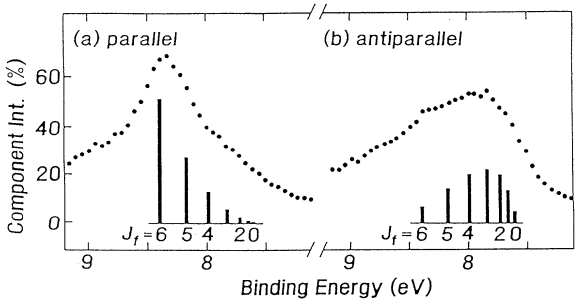

FIG. 3. Vertical bars: Calculated relative intensities of the $4f^6-^7F_J$ final-state multiplet components in the PE spectrum of Gd for (a) parallel ($\Delta M=+1$) and (b) antiparallel ($\Delta M=-1$) orientation of photon spin and sample magnetization. Filled dots: Experimental spectra from Fig. 2, normalized to complete circular polarization.

B. Terbium metal

Terbium, with its many well-resolved $4f$ PE multiplet lines [see Fig. 4(a)] represents an ideal case for the observation of MCD in $4f$ PE. However, Tb metal orders ferromagnetically only below $T_c=220$ K. Since the MCD effect is expected to vanish above T_c and to reach a maximum at saturation magnetization, $M(T)/M(0)=1$, the sample temperature has to be significantly lower than 220 K in order to observe a sizable effect. Because of the relatively large coercivity fields in Tb metal, remanent magnetization could only be achieved by cooling the sample in the presence of an external magnetic field of 400 A/cm from a temperature close to T_c down to the temperature of measurement. This small magnetic field was also found to be sufficient for reversing the film magnetization at temperatures close to T_c, where magnetocrystalline anisotropies and coercivity are small.

Figure 4(a) shows a pair of $4f$ PE spectra from a 150-Å-thick Tb(0001) film at $T=110$ K grown expitaxially on W(110), with parallel and antiparallel orientation of photon spin and sample magnetization. The intensity difference ($I\uparrow\uparrow-I\downarrow\uparrow$), also called "MCD spectrum", is shown in the lower panel [Fig. 4(b), upper curve]. All $4f$ multiplet components reveal nonvanishing MCD, most

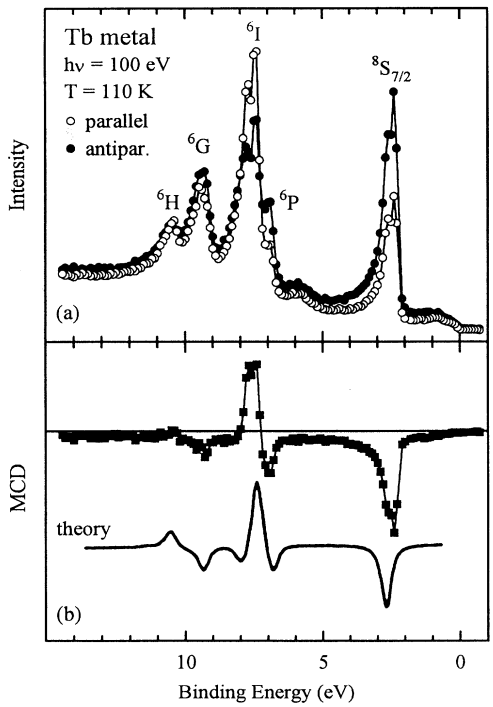

FIG. 4. (a) Tb $4f$ PE spectra ($h\nu=100$ eV) of a remanently magnetized Tb(0001)/W(110) film (150 Å thick; $T=110$ K). Open (filled) dots are for nearly parallel (antiparallel) orientation of photon spin and sample magnetization. (b) Filled squares: Intensity difference (MCD) of the experimental spectra in (a); the solid curve at the bottom of (b) reproduces the theoretical MCD spectrum of Ref. 38.

pronounced for the components with the lowest and the highest orbital angular momenta, respectively. These are the isolated $^8S_{7/2}$ component (with $L=0$) and—with opposite sign—the strong low-spin component, ^6I (with $L=6$). By comparison with the results of the intermediate-coupling calculations of Ref. 38, reproduced in Fig. 4(b) (lower curve), we see that experimental and theoretical MCD curves agree well even in small details.

The isolated high-spin $^8S_{7/2}$ component at a binding energy of $\cong 2.3$ eV deserves further attention. It is separated by more than 4 eV from all the other Tb multiplet components and displays the largest MCD effect of all PE components of Tb (corresponding to an asymmetry of $A_{\text{exp}} \cong 30\%$). For this isolated component, a quantitative comparison with theory is much simpler than for the unresolved ^7F_J multiplet components of Gd. By use of atomic multiplet theory, as described in the previous section, we arrive at an MCD intensity ratio for the Tb-$^8S_{7/2}$ component of 28 to 1; this corresponds to a theoretical asymmetry of $A_{\text{th}}=93\%$. The value refers to the ideal case of fully aligned photon spin and sample magnetization and of completely circularly polarized light. Note that this LS-coupling-scheme result agrees well with the one from intermediate-coupling calculations, where an MCD intensity ratio of 27.7 to 1 was found.[38]

The smaller MCD effect observed experimentally is mainly due to the incomplete circular polarization ($S_3 \cong 0.55$ in the present case) as well as to the relatively high sample temperature of $T=110$ K, corresponding to a reduced temperature of $t=T/T_c \cong 0.5$. For $t=0$ (ferromagnetic ground state), only the lowest-lying magnetic M level would be occupied, i.e., $\langle M \rangle = -J$. Yet, at elevated temperatures, higher M levels get also populated, reducing the MCD effect. For $\langle M \rangle \to 0$, i.e., for equal population of all M levels, the MCD effect is expected to vanish.

We use a spin-wave picture for a qualitative understanding of the influence of temperature on the MCD effect. The $4f$ magnetic moments precess around the sample magnetization giving rise to a perpendicular magnetization component, which will grow with increasing temperature. Since the perpendicular component rotates slowly on the time scale of the PE event, it is seen by the polarized photon as a stationary magnetization component. In the experimental grazing-incidence geometry used here (see Fig. 1), this magnetization component is nearly perpendicular to the photon spin, thus giving rise to $\Delta M=+1$ and $\Delta M=-1$ transitions with equal probability; hereby the net MCD effect gets smaller. We note that with this spin-wave model, the magnitude of the observed MCD effect can be quantitatively described by assuming a circular polarization of $S_3=0.55$, which is a realistic value (see Table I).

C. Dysprosium metal

Dysprosium is the element following Tb in the periodic table and has a $4f^9$ ground-state configuration. Like Tb, bulk Dy assumes ferromagnetic order at low temperatures ($T_c \cong 89$ K). 150-Å-thick Dy(0001) films were grown on W(110). As in the case of Tb metal, they were remanently magnetized by cooling the sample in the presence of an external field from above the highest bulk ordering temperature ($T_N \cong 176$ K) down to the ferromagnetic phase. The MCD-in-$4f$-PE spectra of Dy metal at 55 K are presented in Fig. 5. Despite the fact that the reduced temperature t was only $\cong 0.62$ in the present case, a large MCD effect was observed amounting to an MCD asymmetry of $\cong 25\%$ (not corrected for background) for the shallowest ^7F multiplet component. Note that also other components of the $4f^8$ PE final-state multiplet of Dy exhibit large MCD effects of both signs. The MCD spectrum, calculated from the raw data, is again plotted in (b) and compared with the result of the intermediate-coupling calculation of Ref. 38 (lower solid curve). The agreement between experiment and theory is again very good. Minor deviations stem from the surface-shifted $4f^8$ multiplet and the inelastic background in the PE spectra, which were not considered in the theoretical spectra. Thus Dy provides another favorable case for the study of MCD in $4f$ PE.

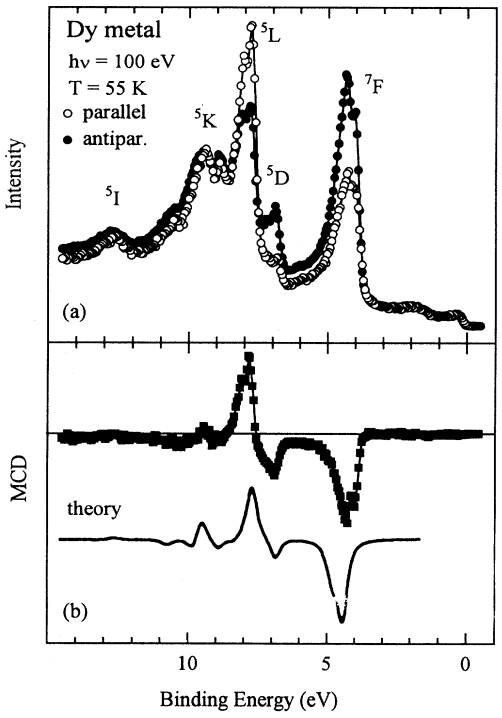

FIG. 5. (a) Dy $4f$ PE spectra ($h\nu=100$ eV) of a remanently magnetized Dy(0001)/W(110) film (150 Å thick; $T=55$ K). Open (filled) dots are for nearly parallel (antiparallel) orientation of photon spin and sample magnetization. (b) Filled squares: Intensity difference of the experimental spectra in (a) (MCD spectrum); the solid curve at the bottom of (b) represents the theoretical MCD spectrum of Ref. 38.

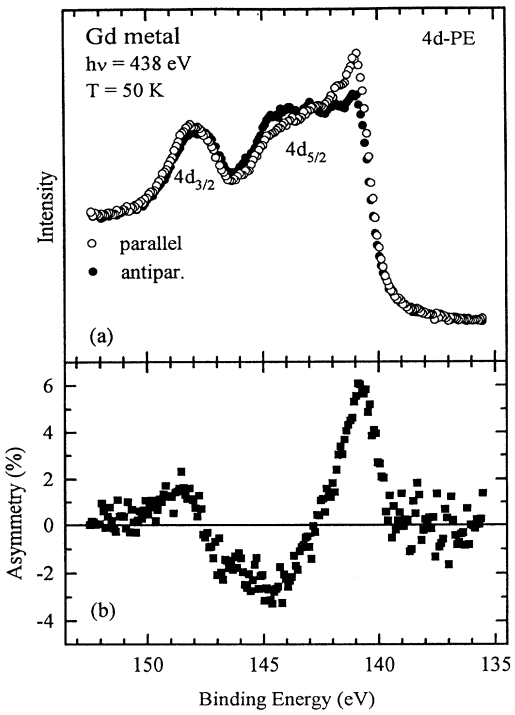

FIG. 6. (a) Gd $4d$ core-level PE spectra ($h\nu=438$ eV) obtained from a remanently magnetized Gd(0001)/W(110) film (80 Å thick; $T=50$ K). Open (filled) dots are for nearly parallel (antiparallel) orientation of photon spin and sample magnetization. The MCD asymmetry derived from the raw data is plotted in (b).

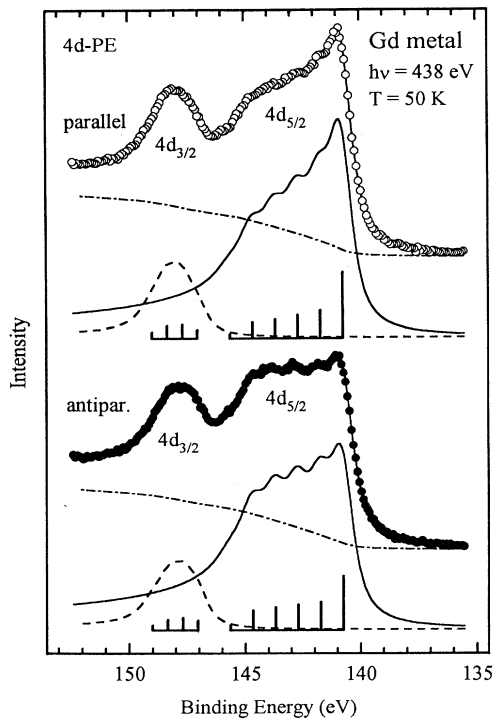

FIG. 7. Results of least-squares fit analysis of the MCD-in-$4d$-PE spectra of Gd metal from Fig. 6(a) by superpositions of 6 (4) equally spaced components for the $4d_{5/2}$ ($4d_{3/2}$) subspectra. For details see text.

IV. MCD IN 4d CORE-LEVEL PHOTOEMISSION FROM Gd METAL

PE from filled lanthanide core levels, like the $4d$ shell of Gd, resembles the case of $2p$ PE from Fe (see the Introduction), where the exchange interaction between core electrons and magnetically ordered electrons is of comparable magnitude as the intrinsic core-hole width;[40] hence one should expect similar MCD effects in the two cases.

We have studied MCD in PE from the $4d$ core levels of Gd in an exploratory way. The results are shown in Fig. 6, where PE spectra, taken at $h\nu=438$ eV, are given for the two orientations of photon spin and sample magnetization. The MCD asymmetry, obtained from the raw data, amounts up to 6% and is plotted in Fig. 6(b). Coming from low binding energies, the asymmetry exhibits a plus-minus feature at the $4d_{5/2}$ subspectrum and a weaker minor-plus feature at the $4d_{3/2}$ subspectrum. Hereby, it resembles indeed the MCD asymmetry observed in core-level PE from the Fe $2p$ level.[21]

A splitting of the $4d_{5/2}$ subspectrum into apparently equally spaced components is visible in the raw data. Accordingly, the $4d$ PE spectra in Fig. 6 were least-squares fitted by a superposition of six equally spaced components for $4d_{5/2}$ and four components for $4d_{3/2}$, with freely varying relative intensities. This accounts for exchange splitting due to $(2J+1)$ orientations of the $4d$-hole angular momentum J with respect to the magnetization direction. Note that this model has only approximate character, since—due to exchange splitting—J can no longer be considered to be a good quantum number.[24] The results of this analysis are shown in Fig. 7 as solid curves through the data points; the dash-dotted curves represent integral backgrounds. As a result, we obtain exchange splittings of 0.98 eV (0.63 eV) between neighboring $4d_{5/2}$ ($4d_{3/2}$) sublevels, and a spin-orbit splitting of $\Delta_{SO}(4d)\cong 4.8$ eV. A complete analysis of the MCD $4d$ core-level PE spectra, using the more appropriate intermediate-coupling scheme, will be given elsewhere.[41]

V. APPLICATIONS

We have shown that MCD in PE from Ln materials can probe magnitude and orientation of the sample magnetization. No time consuming spin analysis of the photoelectrons, as in the established technique of spin-resolved PE, is required. In this way, the new technique can be applied as a "fast" element-specific magnetometer for Ln surfaces and thin magnetic films. On the other hand, the linear dependence of the MCD effect on the degree or circular polarization suggests its use as an x-ray polarimeter. In the following discussion of applications, we shall begin with the latter aspect.

A. X-ray polarimeter

In order to achieve a small reduced temperature $t=T/T_c$, one can either lower the sample temperature or increase T_c, e.g., by alloying Tb with Fe. Intermetallic compounds of the form $TbFe_x$, especially cubic $TbFe_2$ ($T_c\cong 700$ K), have the additional advantage of much smaller magnetocrystalline anisotropies as compared to

Tb metal. We therefore prepared a thin film of $TbFe_x$ by first depositing $\cong 10$ monolayers (ML) Fe onto W(110), followed by $\cong 2$-ML Tb and subsequent annealing. Using LEED, a cubic structure was observed for low electron energies, indicating formation of $TbFe_2$ near the surface of the film. Coercivities were found to be so small that the magnetization at 100 K could be switched by small field pulses as in case of Gd metal.[42]

The $4f$ PE spectra of $TbFe_x$, taken at $h\nu = 152$ eV in $4d \rightarrow 4f$ resonance, are presented in Fig. 8(a). The $^8S_{7/2}$ and ^6I components reveal the largest MCD effect so far observed in PE as well as in x-ray absorption; the intensity asymmetry [see Fig. 8(b)], as calculated from the raw experimental spectra without background subtraction, exceeds 40%. Hardly any MCD effect is noticeable in the emission from Fe $3d$ states close to the Fermi level. Intermixing of Tb and Fe is reflected in the binding energy of the $^8S_{7/2}$ PE line (at $\cong 3.1$ eV), in comparison to that of Tb metal (at $\cong 2.3$ eV).

The isolated $^8S_{7/2}$ component in the PE spectrum of $TbFe_x$ is well suited for measuring—on the basis of MCD—the degree of circular polarization of x rays. Unlike Tb metal, films of the intermetallic compound $TbFe_x$ require only ordinary ultrahigh vacua (in the 10^{-10}-mbar range), and can thus be used for long periods of time. For a first demonstration, we used two different settings of the SX700/III monochromator, accepting synchrotron radiation at angles of $\psi = 0.6$ mrad and $\psi = 0.9$ mrad with respect to the electron-storage-ring plane.

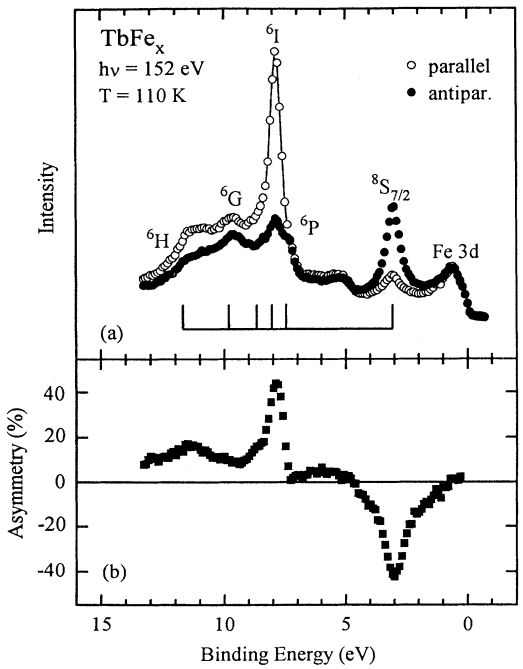

FIG. 8. (a) Tb $4d \rightarrow 4f$ resonant PE spectra ($h\nu = 152$ eV, $T = 110$ K) of a remanently magnetized $TbFe_x$ film grown on W(110). Open (filled) dots are for nearly parallel (antiparallel) orientation of photon spin and sample magnetization. (b) Asymmetry calculated from the raw experimental spectra.

TABLE II. Comparison of experimental results for the degree of circular polarization (in %) of soft x rays from the SX700/III monochromator at BESSY.

$h\nu$ (eV)	0.6 mrad	0.9 mrad	Ref.
70	55		28
152	57±6	69±7	Present work
265	75	90	31

As expected, larger MCD asymmetries were observed for the $\psi = 0.9$-mrad setting. From least-squares fits of the peak intensities, the experimental peak asymmetries A_{exp} were obtained, resulting in (51±5)% for 0.6 mrad and (62±6)% for 0.9 mrad. To extract the degree of circular polarization of the soft x rays (described by the Stokes parameter S_3), one has to consider a correction factor C to account for the nonvanishing angle between light propagation direction and sample magnetization. C is obtained by considering the additional excitation probabilities for $\Delta M = 0, \pm 1$, which are caused by magnetization components perpendicular to the photon spin; $C = 0.96$ in the present case. From the equation $A_{exp} = CS_3 A_{th}$, we obtain $S_3 = (57 \pm 6)\%$ for the $\psi = 0.6$-mrad case and $S_3 = (69 \pm 7)\%$ for 0.9 mrad. Table II shows that these values fit well into the results of optical polarization measurements, since S_3 is known to increase with increasing photon energy at the SX700/III beamline.

B. Surface magnetization

The magnetization of the topmost atomic layer on a Ln-metal surface has attracted considerable attention since the observation of surface-enhanced magnetic order and magnetic-surface reconstruction in 1985, when Weller *et al.* found long-range magnetic order of the surface layer up to some 10 K above the bulk Curie temperature T_c^b, as well as some indication for an antiparallel orientation with respect to the bulk.[43] In order to detect the relative orientation of surface and bulk, they used the surface core-level shift δ_s. In case of Gd metal, the surface and bulk components of the broad ^7F_J multiplet (see Fig. 2) could not be resolved. However, by spin-resolved PE, opposite spin polarizations were observed on the high-binding-energy (surface) side and on the low-binding-energy (bulk) side of the unresolved ^7F_J peak. In a recent repetition of this experiment, with somewhat better statistics and at lower temperatures, the spin polarizations, however, were found to be identical on both sides of the ^7F_J peak, giving thus strong evidence for parallel orientation of surface and bulk.[44]

The very different shapes of the Gd ^7F_J MCD-PE spectra for parallel and antiparallel orientation of magnetization and photon spin (see Fig. 2) suggest readily that this effect should allow to distinguish between parallel and antiparallel orientation of surface and bulk magnetization. In order to enhance the surface contribution, analogous spectra as in Fig. 2 were taken at lower photon energies. Figure 9 shows a pair of MCD-PE spectra of Gd(0001) at

$h\nu = 47$ eV for (a) parallel and (b) antiparallel orientation of sample magnetization (bulk) and photon spin. Both spectra exhibit clearly visible shoulders on the high-binding-energy side, which are a consequence of the intense surface contributions (the surface-to-bulk intensity ratio is $\cong 1.1$); such shoulders had not previously been resolved with unpolarized light.[43–45] In the upper spectrum, which contains predominantly the pointed $\Delta M = +1$ multiplet [compare with Fig. 3(a)], the shoulder is much sharper than in the bottom spectrum, where both the bulk and surface contributions are rounded. This clearly indicates that the magnetizations of surface and bulk are oriented essentially parallel to each other.

For a quantitative description, the two spectra in Fig. 9 were simultaneously least-squares fitted. We used a common parameter set and Doniach-Sunjic line shapes[46] assuming the calculated ^7F_J multiplet intensities (see Sec. IIIA). The resulting spectral shapes were convoluted by a Gaussian to account for finite experimental resolution. For the assumption of parallel alignment of the magnetizations of the (0001) surface layer (grey-shaded components) and of the Gd bulk (solid subspectra), the results are shown as solid curves through the data points in Fig. 9. Assuming antiparallel alignment of surface and bulk or a paramagnetic surface layer, substantial misfits were obtained (not shown here). The MCD data thus clearly rule out antiparallel orientation or lack of long-range magnetic order of the (0001) surface layer. They provide further strong evidence for an essentially parallel magnetic orientation of surface and bulk in case of Gd(0001). This result is corroborated by recent spin-resolved $4f$ PE experiments on thin Gd films[45] as well as by spin analysis of secondary electrons;[47] the latter indicate a nonvanishing normal magnetization component on the Gd(0001) surface in case of relatively thick films, where the bulk properties appear.

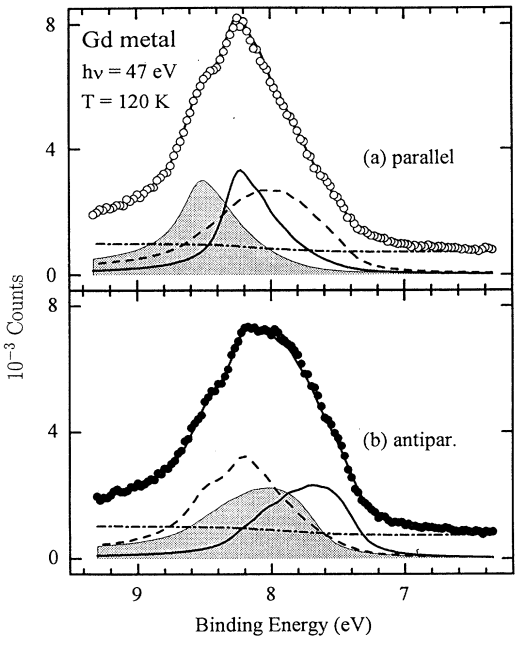

FIG. 9. Surface-sensitive MCD-in-$4f$-PE spectra from Gd(0001)/W(110) for (a) nearly parallel and (b) nearly antiparallel orientation of photon spin and sample magnetization. The spectra show a clear shoulder on the high-binding-energy side due to an intense contribution from the (0001) surface layer. Solid curves through the data points represent least-squares-fit results assuming parallel orientation of surface layer (grey-shaded subspectra) and bulk (solid subspectra). Dashed subspectra summarize bulk and surface transitions with $\Delta M = 0$ and opposite ΔM [$\Delta M = -1$ in (a), $\Delta M = +1$ in (b)] due to incomplete circular polarization, a nonvanishing angle between photon spin and sample magnetization, as well as finite temperature.

An enhancement of the surface Curie temperature had previously also been reported for Tb(0001).[48] On this surface, the isolated $^8S_{7/2}$ $4f$ PE component (see Fig. 4) allows a clear spectroscopic separation of the topmost surface layer from the underlying bulk. Figure 10 displays surface-sensitive MCD-PE spectra in the region of the $^8S_{7/2}$ component of Tb(0001). The PE component is split into a bulk signal at $\cong 2.3$-eV binding energy (BE) and a clearly resolved surface signal, shifted by $\delta_s = (0.26 \pm 0.03)$ eV to higher BE.[49] The well-resolved surface component of the Tb $^8S_{7/2}$ component allows a separate observation of MCD for the surface layer and for the bulk.

The MCD effect is significantly larger for the topmost surface layer than for the bulk, indicating an enhanced in-plane magnetization within the (0001) surface layer. Yet, a quantitative analysis must include the possibilities of (i) a depolarization of the circularly polarized light upon transmission into the bulk and (ii) a changing photoelectron-angular distribution upon reversal of light helicity.[50] The latter would induce an additional intensity variation due to the finite electron-detection angle; both mechanisms are presently investigated in our laboratory.

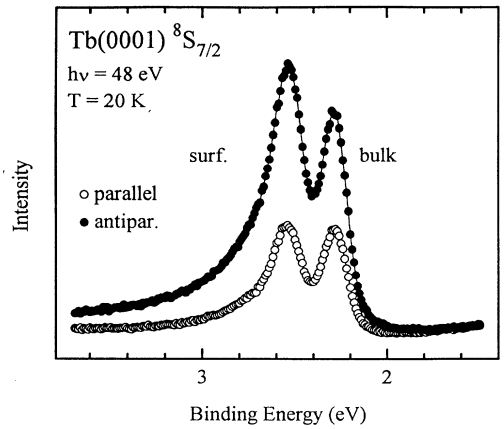

FIG. 10. Surface-sensitive MCD-in-$4f$-PE spectra of Tb(0001). The surface core-level shift of the isolated Tb-$^8S_{7/2}$ PE component allows a separate observation of the MCD effect for the topmost surface layer and for the bulk.

VI. SUMMARY AND PERSPECTIVES

The use of circularly polarized light in PE from ferromagnetically ordered Ln materials leads to very large magnetic circular dichroism (MCD) effects: The intensities of the $4f$ and $4d$ PE components depend strongly on the magnitude and orientation of sample magnetization with respect to the photon spin of the exciting circularly polarized soft x rays. In some relevant cases, like the Tb-$^8S_{7/2}$ $4f$ PE component, the intensity of the $4f$ PE signal is strong for one of the two orientations of magnetization with respect to the photon spin, while it is almost fully quenched for the other orientation (see Fig. 8). MCD in $4f$ PE thus allows to measure the magnetization of a given sample, similar as spin-resolved PE, yet without the need for time-consuming electron-spin analysis.

Due to the localized nature of the $4f$ electrons, MCD in $4f$ PE can be described in an atomic picture. By use of a simple multiplet theory, we can understand the effects as a consequence of the dipole-selection rules. In a few relevant cases (Gd, Tb-$^8S_{7/2}$) one can use the illustrative LS-coupling scheme in conjunction with the dipole selection rules to calculate the MCD effect. The results agree reasonably well with those obtained by more accurate intermediate-coupling calculations.[38]

We suggest to use the MCD-PE asymmetry as an x-ray polarimeter over a wide photon-energy range, from $\cong 30$ eV up to the hard x-ray region, and we give a first demonstration of its feasibility. At the (0001) surface of Ln metals, MCD in $4f$ PE can separate the magnetization within the topmost atomic surface layer from the bulk magnetization, making use of the surface core-level shift. For Gd(0001), it reveals the existence of a large in-plane surface magnetization oriented parallel to the bulk.

MCD in $4f$ PE from magnetically ordered Ln materials opens new perspectives in the analysis of surface and thin-film magnetism: (i) It allows to measure the magnitudes and the relative orientation of bulk and surface magnetizations without the need for electron-spin analysis, i.e., with the speed of conventional PE experiments. In particular, MCD in $4f$ PE can be used to measure the element-specific magnetization in heteromagnetic systems, such as advanced storage media for magneto-optical recording[51] or hard-magnetic materials containing different lanthanides; this will be demonstrated in a forthcoming publication.[52] (ii) The sheer magnitude of the MCD effect is very attractive for domain-imaging applications, offering high magnetic contrast, comparable with or even higher than the one obtained presently by MCD in x-ray absorption.[11] As an advantage, the surface sensitivity is higher and can be varied continuously. This has already motivated first experiments for magnetic imaging.[53] (iii) Exploiting the recently formulated sum-rules,[38] MCD in $4f$ PE has the potential to yield the orbital $4f$ moment, carried by each individual Ln element in, e.g., transition-metal/Ln intermetallic compounds. (iv) $4f$ PE experiments, in which excitation by circularly polarized light is combined with photoelectron-spin analysis, MCD-in-$4f$-PE will directly measure the expectation value of the inner product $\langle \mathbf{L}\cdot\mathbf{S}\rangle$; in such experiments, the orbital angular momentum $\mathbf{L}$ is defined through the circularly polarized light (MCD) and the spin $\mathbf{S}$ through the axis of the electron-spin detector. An experimental access to the strength of $4f$ spin-orbit coupling is important for an improved understanding of the role of single-ion anisotropies in the search for technologically relevant thin magnetic films with perpendicular spontaneous magnetization.

ACKNOWLEDGMENTS

We thank the staff of BESSY, in particular G. Reichart and M. Willmann, for their indispensable experimental help. We are also grateful to G. van der Laan for communicating theoretical MCD multiplet intensities prior to publication and to U. Heinzmann for stimulating discussions. This work was supported by the Bundesminister für Forschung und Technologie, project No. 05-5KEAXI-3/TP01, and the SfB-290/TPA6 of the Deutsche Forschungsgemeinschaft.

[1]G. Schütz, W. Wagner, W. Wilhelm, P. Kienle, R. Zeller, R. Frahm, and G. Materlik, Phys. Rev. Lett. **58**, 737 (1987).

[2]Magnetic *linear* dichroism in the $M_{4,5}$ x-ray-absorption spectra of lanthanide materials had been predicted even earlier by B. T. Thole, G. van der Laan, and G. Sawatzky, Phys. Rev. Lett. **55**, 2086 (1985); this related effect was experimentally demonstrated by G. van der Laan *et al.*, Phys. Rev. B **34**, 6529 (1986).

[3]G. Schütz, M. Knülle, R. Wienke, W. Wilhelm, W. Wagner, P. Kienle, and R. Frahm, Z. Phys. B **73**, 67 (1988).

[4]C. T. Chen, F. Sette, Y. Ma, and S. Modesti, Phys. Rev. B **42**, 726 (1990).

[5]Y. Wu, J. Stöhr, B. D. Hermsmeier, M. G. Samant, and D. Weller, Phys. Rev. Lett. **69**, 2307 (1992).

[6]J. Redinger, C. L. Fu, A. J. Freeman, U. König, and P. Weinberger, Phys. Rev. B **38**, 5203 (1988).

[7]P. Rudolf, F. Sette, L. H. Tjeng, G. Meigs, and C. T. Chen, J. Magn. Magn. Mater. **109**, 109 (1992).

[8]C. T. Chen, Y. U. Idzerda, H.-J. Lin, G. Meigs, A. Chaiken, G. A. Prinz, and G. H. Ho, Phys. Rev. B **48**, 642 (1993).

[9]Y. U. Idzerda, L. H. Tjeng, H.-J. Lin, C. J. Gutierrez, G. Meigs, and C. T. Chen, Phys. Rev. B **48**, 4144 (1993).

[10]An MCD asymmetry of 40% has been reported by J. Tobin *et al.*, Phys. Rev. Lett. **68**, 3642 (1992).

[11]J. Stöhr, Y. Wu, M. G. Samant, B. D. Hermsmeier, G. Harp, S. Koranda, D. Dunham, and B. P. Tonner, Science **259**, 658 (1993).

[12]C. T. Chen, N. V. Smith, and F. Sette, Phys. Rev. B **43**, 6785 (1991).

[13]H. Ebert, P. Strange, and B. L. Gyorffy, Z. Phys. B **73**, 77 (1988).

[14]P. Carra and M. Altarelli, Phys. Rev. Lett. **64**, 1286 (1990).

[15]P. Carra, B. N. Harmon, B. T. Thole, M. Altarelli, and G. A. Sawatzky, Phys. Rev. Lett. **66**, 2495 (1991).

[16]B. T. Thole, P. Carra, F. Sette, and G. van der Laan, Phys. Rev. Lett. **68**, 1943 (1992).

[17]P. Carra, B. T. Thole, M. Altarelli, and X. Wang, Phys. Rev. Lett. **70**, 694 (1994).

[18]C. T. Chen, Y. U. Idzerda, H.-J. Lin, N. V. Smith, G. Meigs, E. Chaban, G. Ho, E. Pellegrin, and F. Sette (unpublished).
[19]U. Fano, Phys. Rev. **178**, 131 (1969).
[20]G. Schütz, Phys. Bl. **46**, 475 (1990).
[21]L. Baumgarten, C. M. Schneider, H. Petersen, F. Schäfers, and J. Kirschner, Phys. Rev. Lett. **65**, 492 (1990).
[22]C. M. Schneider, D. Venus, and J. Kirschner, Phys. Rev. B **45**, 5041 (1992).
[23]C. Boeglin, E. Beaurepaire, U. Schorsch, B. Carriere, K. Hricovini, and G. Krill, Phys. Rev. B **48**, 13 123 (1993).
[24]H. Ebert, L. Baumgarten, C. M. Schneider, and J. Kirschner, Phys. Rev. B **44**, 4406 (1991).
[25]C. M. Schneider, M. S. Hammond, P. Schuster, A. Cebollada, R. Miranda, and J. Kirschner, Phys. Rev. B **44**, 12 066 (1991).
[26]J. Bansmann, M. Getzlaff, C. Westphal, F. Fegel, and G. Schönhense, Surf. Sci. **269/279**, 622 (1992).
[27]J. K. Lang, Y. Baer, and P. A. Cox, J. Phys. F **11**, 121 (1981).
[28]H. Petersen, M. Willmann, F. Schäfers, and W. Gudat, Nucl. Instrum. Methods Phys. Res. Sect. A **333**, 594 (1993).
[29]J. Bahrdt, A. Gaupp, W. Gudat, M. Mast, K. Molter, W. B. Peatman, M. Scheer, Th. Schroeter, and Ch. Wang, Rev. Sci. Instrum. **63**, 339 (1992).
[30]M. Born and E. Wolf, *Principles of Optics* (Pergamon, London, 1959).
[31]S. Di Fonzo, W. Jark, F. Schaefers, H. Petersen, A. Gaupp, and J. H. Underwood, Appl. Optics **33**, 2624 (1994).
[32]B. J. Beaudry and K. A. Gschneidner, in *Handbook on the Physics and Chemistry of Rare Earths,* edited by K. A. Gschneidner and L. R. Eyring (North-Holland, Amsterdam, 1978), Vol. 1, Chap. 2.
[33]J. Kolaczkiewicz and E. Bauer, Surf. Sci. **175**, 487 (1986).
[34]M. Farle, K. Baberschke, U. Stetter, A. Aspelmeier, and F. Gerhardter, Phys. Rev. B **47**, 11 571 (1993).
[35]B. T. Thole and G. van der Laan, Phys. Rev. B **49**, 9613 (1994).
[36]K. Starke, K. Ertl, and V. Dose, Phys. Rev. B **46**, 9709 (1992).
[37]K. Starke, E. Navas, L. Baumgarten, and G. Kaindl, Phys. Rev. B **48**, 1329 (1993).
[38]G. van der Laan and B. T. Thole, Phys. Rev. B **48**, 210 (1993).
[39]R. D. Cowan, *Theory of Atomic Spectra and Structure* (University of California Press, Berkeley, 1981).
[40]S. P. Kowalczyk, N. Edelstein, F. R. McFeely, L. Ley, and D. A. Shirley, Chem. Phys. Lett. **29**, 491 (1974).
[41]G. van der Laan, E. Arenholz, E. Navas, A. Bauer, and G. Kaindl (unpublished).
[42]K. Starke, L. Baumgarten, E. Arenholz, E. Navas, and G. Kaindl, Phys. Rev. B **50**, 1317 (1994).
[43]D. Weller, S. F. Alvarado, W. Gudat, K. Schröder, and M. Campagna, Phys. Rev. Lett. **54**, 1555 (1985).
[44]G. A. Mulhollan, K. Garrison, and J. L. Erskine, Phys. Rev. Lett. **69**, 3240 (1992).
[45]E. Vescuvo, C. Carbone, and O. Rader, Phys. Rev. B **48**, 7731 (1993).
[46]S. Doniach and M. Sunjic, J. Phys. C **3**, 285 (1970).
[47]H. Tang, D. Weller, T. G. Walker, J. C. Scott, C. Chappert, H. Hopster, A. W. Pang, D. S. Dessau, and D. P. Pappas, Phys. Rev. Lett. **71**, 444 (1993).
[48]C. Rau, Appl. Phys. A **49**, 579 (1989).
[49]E. Navas, K. Starke, C. Laubschat, E. Weschke, and G. Kaindl, Phys. Rev. B **48**, 14 753 (1993).
[50]Y. U. Idzerda and D. E. Ramaker, in *Magnetic Ultrathin Films: Multilayers and Surfaces/Interfaces and Characterization,* edited by B. T. Jonker, S. A. Chambers, R. F. C. Farrow, C. Chappert, R. Clarke, W. J. M. de Jonge, T. Egami, P. Grünberg, K. M. Krishnan, E. E. Marinero, C. Rau, and S. Tsunashima, MRS Symposia Proceedings No. 313 (Materials Research Society, Pittsburgh, 1993), p. 659.
[51]J. Daval and B. Bechevet, J. Magn. Magn. Mater. **129**, 98 (1994).
[52]E. Arenholz, E. Navas, K. Starke, and G. Kaindl (unpublished).
[53]T. Kachel, W. Gudat, and K. Holldack, Appl. Phys. Lett. **64**, 655 (1994).